

Rietveld refinement, electrochemical and CW laser-induced third-order NLO properties of (Mg⁺Ag) and (Mg+Li) doped thin films of CdO

R. Ganapathi*, T. Arivudainambit†, S. Sakthivel‡, A.R. Balu‡

Abstract

Thin films of CdO doped with (Mg+Ag) and (Mg+Li) were spray deposited. Rietveld refined XRD patterns confirmed the cubic nature of the deposited films. Crystallite sizes were 29 and 24 nm for the (Mg+Ag) and (Mg+Li) thin films, respectively. The third-order nonlinear absorption of both films exhibits reverse saturable absorption due to two-photon absorption, and they have high refractive indices. Compared to (Mg+Ag), the (Mg+Li)-codoped film exhibits a high susceptibility of 4.39×10^{-6} esu due to the localised electric-field effect induced by Li⁺ ion incorporation. The enhanced nonlinear optical behaviour observed in the (Mg+Li)-codoped film makes it potentially suitable for optical switching devices. The presence of anodic and cathodic peaks demonstrates the pseudocapacitive nature of MA and ML. The specific capacitance (C_s), charge transfer resistance (R_{CT}) values were estimated to be 123.6 F/g, 92.8×10^3 ohms and 189.2 F/g, 47.4×10^3 ohms for (Mg+Ag) and (Mg+Li) thin films,

* Department of Physics, Kamadhenu College of Arts & Science, Dharmapuri, Tamil Nadu, India; ganapathiraja.1986@gmail.com

† PG and Research Department of Physics, Rajah Serfoji Govt College (Affiliated to Bharathidasan University, Tiruchirappalli), Thanjavur, Tamil Nadu, India; nambita41@gmail.com; Sakthivelphysics464@gmail.com

‡ PG and Research Department of Physics, AVVM Sri Pushpam College (Affiliated to Bharathidasan University, Tiruchirappalli), Poondi, Tamil Nadu, India; arbalu757@gmail.com

respectively. Increased C_S and R_{CT} values realized for the (Mg+Li) codoped film confirmed its utility in electrochemical devices, especially as a pseudocapacitor.

Keywords: Spray pyrolysis; Z-scan; optical switching; electrochemical; pseudocapacitor

1. Introduction

Nanoscale functional materials with enhanced optical and electrochemical properties are required for the design and fabrication of efficient, miniaturised optical and energy-storage devices [1]. Metal oxide thin films have attracted broad attention due to their exceptional properties, such as a large band gap, quantum confinement, high surface area, and stability [2], which are influenced by their size and shape. Metal oxides with strong nonlinear optical properties are effective in applications such as optical memory, optical limiting devices, optical computers, and all-optical switching elements used in photonics [3]. Metal oxides have been a subject of interest in electrochemistry due to their low cost, efficiency, versatility, and unique physicochemical features. Among the metal oxides, cadmium oxide (CdO) is promising for optical devices due to its high transparency, low electrical resistivity, high mobility, and good thermal, chemical, and mechanical stability [4]. In nonlinear optical devices, CdO's defects and surface traps provide new channels for photon absorption and emission, thereby altering its electronic structure [5]. The native defects of CdO (cadmium interstitials (Cd_i) and oxygen vacancies (V_o)) contribute to high electrical conductivity through the formation of Vo^+ defect centres, which capture electrons [6].

However, the non-stoichiometric character in CdO during synthesis limits its light-absorbing properties, thereby reducing the efficiency of CdO-based optical devices. This demerit could be rectified by regulating CdO's native defects, which could be achieved by doping with either cationic or anionic impurities, or by simultaneously incorporating both. In our earlier work, CdO has been doped with magnesium to improve its optical, electrical and optoelectronic properties [4]. But, even at high Mg doping concentration (8 at. %), the obtained resistivity value is high ($0.0853 \times 10^1 \Omega\text{-cm}$) compared to pure CdO. Hence, to improve its electrical conductivity, double doping has been attempted using Mg as a cationic dopant and Ag/Li as the other dopant. Both Ag and Li enhance carrier ion mobility by lowering solution viscosity, thereby improving the conductivity of CdO:Mg, minimising recombination centres through passivation, and preventing electron trapping. Hence, the simultaneous incorporation of Mg, Ag and Mg, Li in CdO is likely to produce noteworthy

outcomes for applications in optical switching and electrochemical devices. Table 1 summarises the works performed earlier on CdO-based materials along with their properties enhanced.

Table 1: Recent works on CdO-based materials

Material	Sample form	Preparation technique	Properties enhanced	Reference
Ag+Co codoped CdO	Thin film	Spray pyrolysis	Optoelectronic	[7]
CdO	Thin film	Nebuliser spray pyrolysis	Gas sensing	[8]
CdO	Thin film	Spray pyrolysis	Optical	[9]
CdO:Co	Thin film	SILAR	Optical and electrical	[10]
CdO	Thin film	Nebuliser spray pyrolysis	Gas sensing	[11]
CdO:Cs	Thin film	Spray pyrolysis	Optical	[12]

The present work aims to improve CdO's optical absorption, electronic structure and electrochemical nature by codoping with (Mg+Ag) and (Mg+Li). The films were prepared by the spray pyrolysis technique, which is user-friendly, cost-effective, capable of large-area coating, and allows easy manipulation of spray parameters such as spray-to-nozzle distance, deposition temperature, spray interval, etc. The spray parameters used in this work are: Deposition temperature - 400°C, substrate - micro glass slides, solvent volume - 50 mL, substrate to nozzle distance - 25 cm, spray angle - 45°, spray interval - 2 sec and spray rate - 6 mL/min. Z-scan and CV studies were performed to evaluate the NLO and electrochemical properties of the films. Comparative analysis of the electrochemical and nonlinear optical properties of (Mg+Ag)- and (Mg+Li)- double-doped CdO thin films is very scarce in the literature.

2. Experimental details

Cadmium acetate (0.1 M), magnesium chloride (2 wt% optimized value), 2 wt% of silver nitrate and lithium chloride are the salts used to deposit (Mg+Ag) and (Mg+Li) codoped CdO thin films [13]. To deposit (Mg+Ag) codoped CdO (MA) thin film, cadmium acetate, magnesium chloride and silver nitrate dissolved in 50 mL of water were sprayed at 400°C on glass substrates. To deposit a (Mg+Li)-codoped CdO (ML) thin film, silver nitrate is replaced with lithium chloride in the above-mentioned solution, and the solution is sprayed. The thicknesses of the films measured with the Stylus profilometer were 384 and 367 nm for the MA and ML thin films, respectively. The films were characterised by X'Pert PRO Analytical X-ray diffractometer and HITACHI S-3000 H microscope. Z-scan studies were performed using a TM215-50 Z-scan system operated with a Nd-YAG laser. An EG & G 273 workstation, which uses Pt, (Mg+Ag), (Mg+Li)-codoped CdO, and a saturated calomel electrode (SCE) as the counter, testing, and reference electrodes, was used to perform CV studies with 0.1 M KOH as the electrolyte.

3. Discussion of the Results

3.1 XRD

XRD patterns of MA and ML thin films (Figure 1) confirmed the cubic structure of CdO (JCPDS Card No. 05-0640).

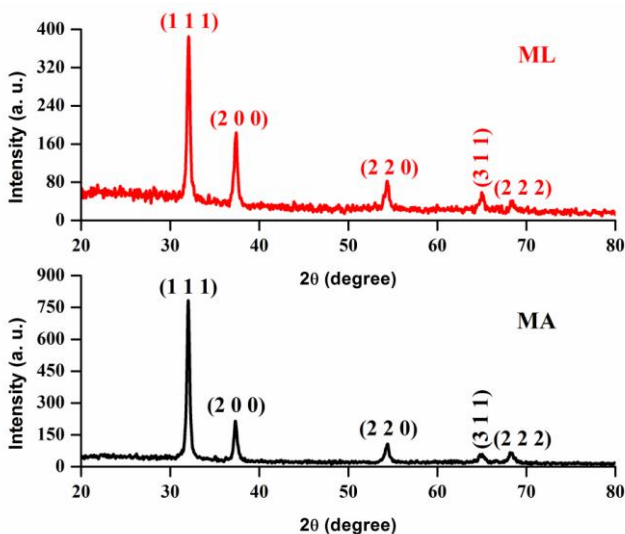


Figure 1: MA and ML's XRD patterns

The absence of impurity related peaks corresponding to Mg, Ag and Li in the XRD patterns confirmed the purity of the as-deposited films. Both MA and ML thin films exhibited a (1 1 1) preferential orientation, as evidenced by the Rietveld XRD patterns (Figure 2). The microstructural parameters were calculated using the formulae [14].

$$\text{Crystallite size, } D = \frac{0.9\lambda}{\beta \cos\theta} \quad (1)$$

$$\text{Strain, } \varepsilon = \frac{\beta \cot\theta}{4} \quad (2)$$

$$\text{Dislocation density, } \delta = \frac{1}{D^2} \quad (3)$$

$$\text{Lattice constant, } a = \frac{d}{\sqrt{h^2+k^2+l^2}} \quad (4)$$

where θ - Bragg's angle and β - FWHM of the (1 1 1) peak.

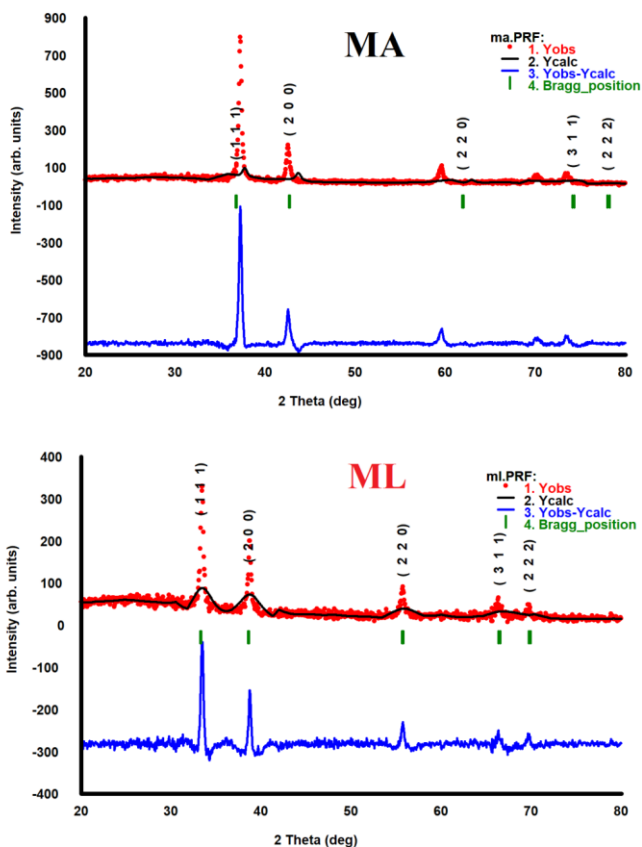


Figure 2: MA and ML's Rietveld refined XRD patterns

The obtained structural and Rietveld refined parameters are compiled in Table 2.

Table 2: MA and ML’s microstructural and Rietveld refined parameters

Film	Microstructural parameters			Rietveld refined parameters				
	D (nm)	Strain, $\epsilon \times 10^{-3}$	Dislocation density, $\delta \times 10^{-15}$	Lattice constant, a (Å)	R _p	R _{wp}	R _e	χ^2
MA	29	4.768	1.189	4.8396	157	103	29.1	12.46
ML	24	5.222	1.736	4.8287	36.6	42.3	23.2	3.344

3.2 SEM

MA and ML’s SEM images (Figure 3) confirmed uniform distribution of grains, with grain sizes being equal to 86.4 and 48.6 nm, respectively. ML’s reduced grain size compared with MA agrees with the XRD results.

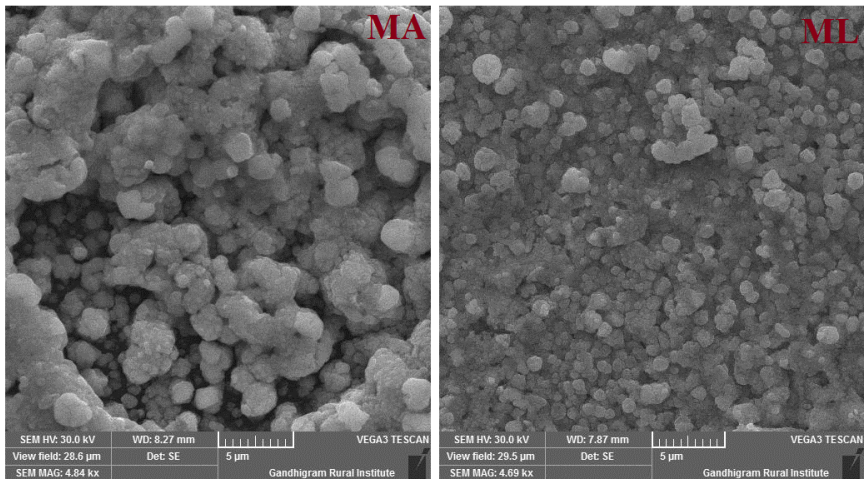


Figure 3: MA and ML’s SEM images

3.3 Z-scan studies

Closed aperture curves of MA and ML thin films (Figure 4) displayed a peak followed by valley signifying -ve refractive index due to self-defocusing process [15].

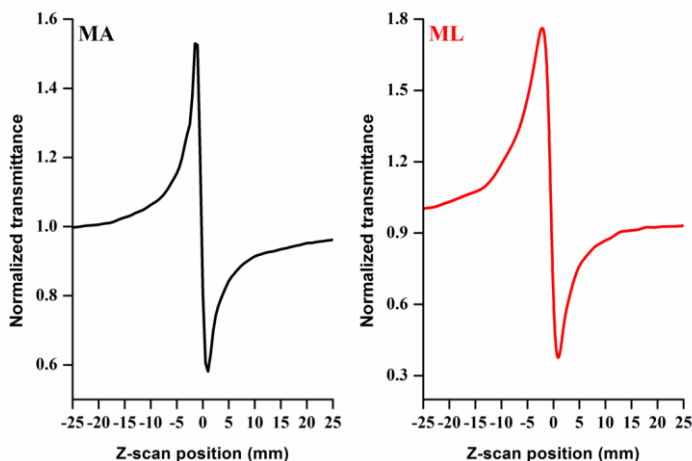


Figure 5: MA and ML's open aperture curves

The nonlinear optical parameters (refractive index (n_2), absorption coefficient (β) and susceptibility (χ^3)) values obtained for MA and ML films compiled in Table 3 showed that ML exhibited better nonlinear optical properties.

Table 3: MA and ML's NLO parameters

Film	NLO parameters		
	Refractive index $n_2 \times 10^{-9} \text{ cm}^2/\text{W}$	Absorption coefficient $\beta \times 10^{-4} \text{ cm}/\text{W}$	Susceptibility $\chi^3 \times 10^{-6} \text{ (esu)}$
MA	3.29	2.76	2.28
ML	5.38	3.19	4.39

Possible reasons might be: i) High polarizability and minimum cationic field strength of Li^+ ions compared to Ag^+ ions, ii) Compared to Ag^+ , Li^+ ions possess lower electronic energy loss during irradiation, iii) due to smaller ionic radius compared to Ag^+ (1.15\AA), Li^+ (0.76\AA) ions could occupy substitutional sites of $\text{CdO}:\text{Mg}$ matrix in plenty contributing more electrical conductivity, iv) Li^+ has a very high charge density and hydration energy compared to Ag^+ . Due to improved nonlinear optical properties, ML film is well-suited for optical switching devices.

3.4 Electrochemical

The CV Profiles of MA and ML performed at different scan rates (10, 30,

50 and 100 mV/s) shown in Figure 6(a, b) confirmed the presence of anodic and cathodic peaks supporting their pseudo-capacitive nature. The current response observed for both MA and ML was nonlinear with the scan rate, indicating that adsorption- and diffusion-controlled processes occur in the electrochemical reaction [17]. With increasing scan rate, the current response curve increases for both MA and ML. The quasi-rectangular form observed is caused by the Faradaic reversible redox reaction [18].

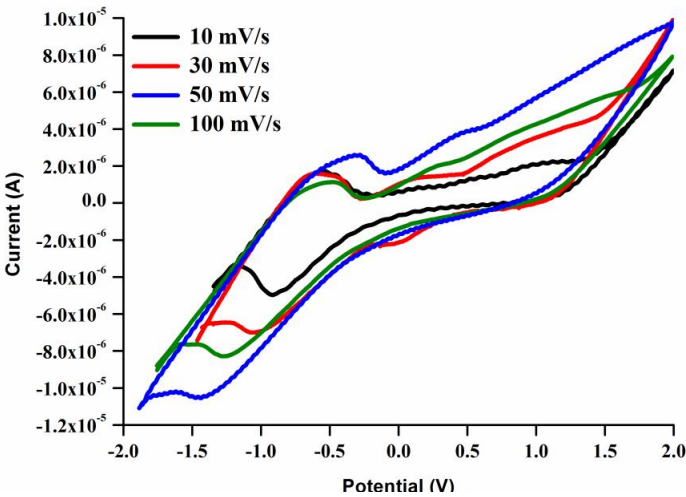


Figure 6 (a): MA's CV curves

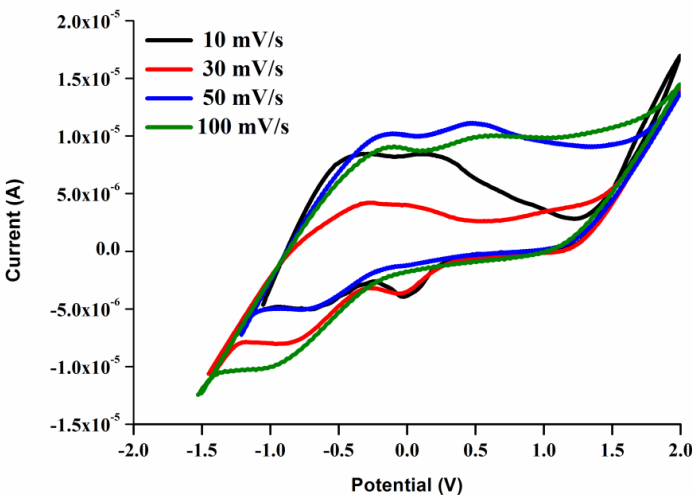


Figure 6 (b): ML's CV curves

The specific capacitance (C_s) values calculated using the relation, $C_s = \frac{\int Idv}{\Delta v m s}$ (where $\int Idv$ is the integrated CV curve area, m is the active mass (mg), Δv is the potential window and s is the scan rate) were 123.6 and 189.2 F/g for MA and ML, respectively. The increased ML's C_s value might be due to the high charge density of Li^+ ions compared to Ag^+ ions and hence more ion diffusion or charge transfer takes place at the interface of electrode-electrolyte.

The charge transfer resistance R_{CT} resulting from the redox reaction and double layer capacitance occurring on the surface of MA and ML were calculated from the diameter of the semicircle in the Nyquist plots (Figure 7) whose equivalent circuit is displayed in Figure 8.

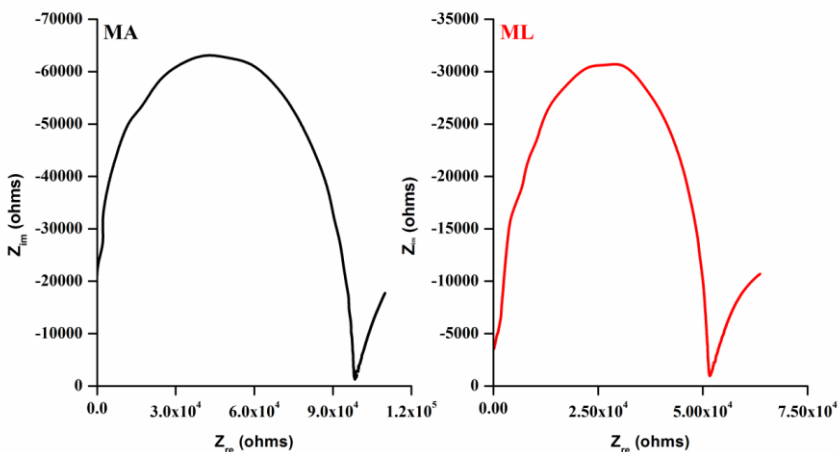


Figure 7: MA and ML's Nyquist plots

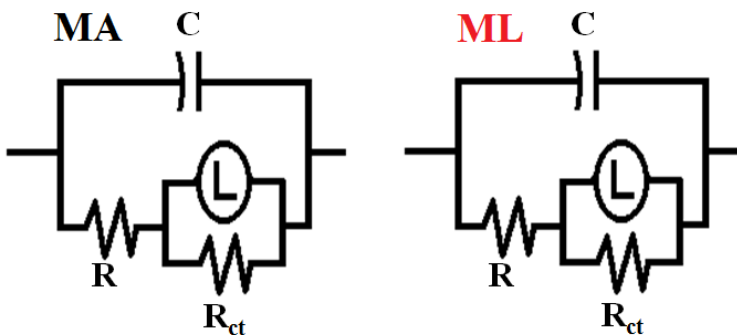


Figure 8: Equivalent circuit diagram for MA and ML's Nyquist plots

The R_{CT} values were 92.8 and 47.4×10^3 ohms for MA and ML, respectively. ML's potential as a supercapacitor was validated by its lowest R_{CT} value.

Conclusion

Spray-deposited (Mg+Ag)- and (Mg+Li)- doped CdO films exhibited preferential (1 1 1) growth. ML exhibited a higher nonlinear refractive index ($5.38 \times 10^{-9} \text{ cm}^2/\text{W}$), absorption coefficient ($3.19 \times 10^{-4} \text{ cm/W}$) and susceptibility ($4.39 \times 10^{-6} \text{ esu}$) compared to that of MA. These qualities make ML film well-suited for optical switching devices. Electrochemical analysis of ML confirmed its excellent charge-discharge characteristics. ML exhibited a low R_{CT} value of $47.4 \times 10^3 \text{ ohms}$ compared to MA ($92.8 \times 10^3 \text{ ohms}$). A high specific capacitance of 189.2 F/g was obtained for ML, confirming its utility as an efficient electrode material for pseudocapacitors.

Statements & Declarations

Conflict of Interest

No conflict of interest exists in the article.

Funding

The authors confirm that they received no grants, funds, or other forms of assistance in preparing this manuscript.

Acknowledgements

Mr Vincent of St. Joseph's College, Trichy, Tamil Nadu is very much thanked for the CV studies.

References

- [1] K. A. Ann Mary, N.V. Unnikrishnan and R. Philip, *Physica E*. 74, 151 – 155 (2015). <https://doi.org/10.1016/j.physe.2015.06.031>.
- [2] M. Shkir, M. Arif, V. Ganesh, M.A. Manthrammel, A. Singh, S.R. Maidur, P.S. Patil, I.S. Yahia, H. Algarni and S. Alfaify, *J. Mater. Res.* 33, 3880 – 3889 (2018). <https://doi.org/10.1557/jmr.2018.310>.
- [3] M. Shahmiri, N.A. Ibrahim, N. Faraji, W.M.M. Yunus, N. Asim and N. Zainuddin, *Physica E*. 54, 109 – 114 (2013). <https://doi.org/10.1016/j.physe.2013.06.014>.
- [4] K. Usharani, A.R. Balu, V.S. Nagarethinam and M. Suganya, *Prog. Nat. Sci.* 25, 251 – 257 (2015). <https://doi.org/10.1016/j.pnsc.2015.06.003>.

- [5] N. Manjula, A.R. Balu, K. Usharani, N. Raja, V.S. Nagarethinam, *Optik*. 127, 6400 – 6406 (2016). <https://doi.org/10.1016/j.ijleo.2016.04.129>.
- [6] R. Halabi, A.M. Abdallah, M.I. Khalil, R. Awad and M. Mattar, *Appl. Phys. A*. 129, 307 (2023). <https://doi.org/10.1007/s00339-023-06606-0>.
- [7] I. Karim, M.A.H. Naeem, A.S.R. Ayon, Md.A. Sattar, Md.A. Sabur, A.N. Ahmad, *Mater. Adv.* 6, 703 (2025). <https://doi.org/10.1039/D4M A00918E>.
- [8] V. Vijayanarayanan, V. Arivindan, B. Karuppasamy, *Physica Scripta*, 99, 085979 (2024), <https://doi.org/10.1088/1402-4896/ad623f>.
- [9] R.S. Meshram, V.R. Panse, S.M. Waghare, A. Manap, A. Hadap, A. Saregar, *J. Optics*, (2024). <https://doi.org/10.1007/s.12596-024-02437-1>.
- [10] T.C. Tasdemirci, *Mater. Chem. Phys.* 346, 131320 (2025). <https://doi.org/10.1016/j.matchemphys.2025.131320>.
- [11] B. Amudhavalli, M. Ramasamy, P. Manivannan, R.N. Jayaprakash, *J. Mater. Sci. Mater. Electron.* 35, 547 (2024). <https://doi.org/10.1016/s10854-024-12240-0>.
- [12] S.T. Aldabag, *AIP Conf. Proc.* 3486, 050001 (2026). <https://doi.org/10.1063/1.20042837>.
- [13] R. Ganapathi, T. Arivudainambi, S. Sakthivel, A.R. Balu, *J. Optoelectron. Biomedical Mater.* 18, 85 (2026). <https://doi.org/10.15251/JOBM.2026.181.85>.
- [14] M. Barzegar, D. Ahmadvand, Z. Sabouri and M. Darroudi, *Mater. Res. Bull.* 169, 112514 (2024). <https://doi.org/10.1016/j.materresbull.2023.112514>.
- [15] K. Devendran, A.R. Balu, Z. Delci, N. Arunkumar, S. Chithra Devi, M. Suganya, V. Rajamani and A. Vinith, *Ceram. Int.* 51, 14767 – 14777 (2025). <https://doi.org/10.1016/j.ceramint.2025.01.319>.
- [16] C. Rajashree, A.R. Balu, N. Arunkumar, Z. Delci, C. Kayathiri, M. Karthika, K. Devendran, V. Rajamani, M. Sriramraj and A. Vinith, *J. Alloys Compnd.* 1035, 181481 (2025). <https://doi.org/10.1016/j.jallcom.2025.181481>.
- [17] Q. Jiang, N. Kumar, M. Alhabeab, Y. Gogotsi and H. Alshareef, *Adv. Energy Mater.* 8, 1703043 (2018). <https://doi.org/10.1002/aenm.201703043>.
- [18] M. Suganya, A.R. Balu, B. Sowmiya Devi, S. Chithra Devi, M. Karthika, C. Kayathiri, M. Sriramraj, K. Devendran and S. Adityan, *J. Clust. Sci.* 35, 827 – 843 (2024). <https://doi.org/10.1007/s10876-023-02522-8>.